Accumulation of Caveolin in the Endoplasmic Reticulum Redirects the Protein to Lipid Storage Droplets

Anne G. Ostermeyer,* James M. Paci,* Youchun Zeng,‡ Douglas M. Lublin,‡ Sean Munro,§ and Deborah A. Brown*

*Department of Biochemistry and Cell Biology, State University of New York at Stony Brook, Stony Brook, New York 11794; ‡Department of Pathology, Washington University School of Medicine, St. Louis, Missouri 63110; and §Medical Research Council Laboratory of Molecular Biology, Cambridge CB2 2QH, United Kingdom

Abstract. Caveolin-1 is normally localized in plasma membrane caveolae and the Golgi apparatus in mammalian cells. We found three treatments that redirected the protein to lipid storage droplets, identified by staining with the lipophilic dye Nile red and the marker protein ADRP. Caveolin-1 was targeted to the droplets when linked to the ER-retrieval sequence, KKSL, generating Cav–KKSL. Cav–ΔN2, an internal deletion mutant, also accumulated in the droplets, as well as in a Golgi-like structure. Third, incubation of cells with brefeldin A caused caveolin-1 to accumulate in the droplets. This localization persisted after drug washout, showing that caveolin-1 was transported out of the droplets slowly or not at all. Some overexpressed caveolin-2 was also present in lipid droplets. Experimental reduction of cellular cholesteryl ester by 80% did not prevent targeting of Cav–KKSL to the droplets. Cav–KKSL expression did not grossly alter cellular triacylglyceride or cholesteryl levels, although droplet morphology was affected in some cells. These data suggest that accumulation of caveolin-1 to unusually high levels in the ER causes targeting to lipid droplets, and that mechanisms must exist to ensure the rapid exit of newly synthesized caveolin-1 from the ER to avoid this fate.

Key words: caveolae • brefeldin A • retrograde transport • triacylglycerol • cholesteryl ester

Introduction

Caveolae, 50–100-nm plasma membrane pits, have been implicated in functions as diverse as signal transduction, cholesterol transport, and endocytosis (Kurzchalia and Parton, 1999; Smart et al., 1999). A useful approach to understanding caveolae is to study caveolin-1, an important structural protein of caveolae that is required for their formation (Fra et al., 1995). The mammalian caveolin gene family also includes the widely expressed caveolin-2 and the muscle-specific caveolin-3 (Smart et al., 1999).

Caveolin-1 has been proposed to move from the ER through the cytosol directly to the plasma membrane, in a complex with molecular chaperones, as part of an unusual intracellular cycling itinerary (Uittenbogaard et al., 1998). The present study was initiated to test this idea. Resident ER membrane proteins that escape from the ER are efficiently retrieved through recognition of a KKXX signal on their COOH termini by the COPI complex (Letourneur et al., 1994). We appended the sequence KKSL to the COOH terminus of Myc-tagged canine caveolin-1, generating Cav–KKSL. We reasoned that if caveolin-1 must traverse the ER–Golgi intermediate complex and Golgi apparatus after leaving the ER, then Cav–KKSL, like other KKXX-tagged proteins, would not reach the plasma membrane. Alternatively, if some caveolin-1 moved directly from the ER to the plasma membrane, it would bypass the retrieval compartments and accumulate in the plasma membrane.

As described here, we found essentially no Cav–KKSL in the plasma membrane, suggesting that the protein always entered the retrieval compartments. However, instead of being restricted to the ER, Cav–KKSL displayed a novel localization to large round structures that we found were lipid storage droplets.

Eukaryotic cells store neutral lipids in cytoplasmic droplets (Londos et al., 1999; Murphy and Vance, 1999). Although formation of these droplets is especially well developed in adipocytes and in certain plant cells, they are present in a variety of mammalian cell types. Lipid droplets bud from the ER, and are thought to be surrounded by a phospholipid monolayer enriched in certain proteins. Adipocyte differentiation related protein

(ADRP),[1] which has a wide tissue distribution in animal cells, is among the best characterized of these. ADRP associates specifically with lipid storage droplets, and not with the ER from which the droplets are derived, and is thus a useful marker of the droplets (Londos et al., 1999).

Localization of Cav–KKSL to these droplets was surprising, as endogenous caveolin-1 is never seen there. Characterizing this localization became the focus of this project.

Materials and Methods

Materials

Fischer rat thyroid (FRT) cells (Lipardi et al., 1998), the gift of Dr. Enrique Rodriguez-Boulan (Cornell University, Ithaca, New York), were maintained in Coon's F12 media with 10% FBS. COS, CHO, and HEK 293 cells (American Type Culture Collection) were maintained in DME with 5% iron-supplemented calf serum or 10% FBS.

All caveolin-1 constructs were derived from canine caveolin-1 (VIP21; Kurzchalia et al., 1992). HA/myc-tagged caveolin-1 has been described (Dietzen et al., 1995). Cav–ΔN2, lacking residues T46–T95, was generated from HA/myc-tagged caveolin-1 by PCR. Plasmid SAV2MK1 (derived from SMH3, a COS cell expression vector with an adenovirus major late promoter) encodes caveolin-1 with the COOH-terminal extension GVD-MEQKLISEEDLNSKKSL, including a myc tag and then KKSL. The control plasmid, SAV2M2, lacked the COOH-terminal KKSL. A GFP-tagged caveolin-1 cDNA was constructed by subcloning the HA/myc-tagged caveolin-1 as a 0.6-kb XhoI/ApaI fragment (Dietzen et al., 1995) into the same sites in pEGFP-C1 (CLONTECH), yielding an in-frame fusion with GFP at the NH_2 terminus of caveolin-1. Human caveolin-2 from an EST clone (GenBank/EMBL/DDBJ accession no. AA150110) from Research Genetics was cloned by PCR into pCGN (Tanaka and Herr, 1990) to fuse an HA epitope tag to the NH_2 terminus of the protein.

Transient transfections used Lipofectamine 2000, Lipofectamine Plus (Life Technologies), or Fugene 6 (Roche), examining cells 24–48 h after transfection. FRT cells were stably transfected using calcium phosphate, selecting with G418.

Antibodies

Antibodies used: rabbit anti–caveolin-1 antibodies (#13630, BD Transduction Laboratories). Mouse anti-HA IgG (clone 12CA5) was the gift of Dr. Neta Dean (SUNY Stony Brook, Stony Brook, NY). Mouse anti-myc IgG (Invitrogen). Mouse anti-ADRP (ProGen). Dichlorotriazinylaminofluorescein (DTAF)- and Texas red-conjugated goat–anti rabbit and anti–mouse IgG (Jackson ImmunoResearch).

Pfizer's acyl CoA:cholesterol acyl transferase (ACAT) inhibitor CP 113,818 (Warner et al., 1995) was the gift of Dr. George Rothblat (Children's Hospital of Philadelphia, Philadelphia, PA). Brefeldin A (BFA), Nile red, and FITC-conjugated lens lectin were from Sigma Chemical Co.

Fluorescence Microscopy

Immunofluorescence (IF) microscopy was as described (Arni et al., 1998), except that cells used for Nile red staining were permeabilized for 5 s on ice in PBS/0.05% Triton X-100. Fluorescent images of cells were captured into Adobe Photoshop from a SPOT cooled CCD 24 bit color digital camera (Diagnostic Instruments) mounted on a Zeiss Axioskop 2 microscope. For double labeling, images in two channels were collected separately and then overlaid in Photoshop. Where appropriate, coverslips were incubated with 100 nM Nile red in PBS for 10 min. Nile red was detectable in both DTAF and Texas red channels. Double labeling with DTAF was possible because the Nile red staining bleached rapidly. After collection of Nile red images, the Nile red fluorescence was completely bleached to reveal the DTAF fluorescence.

---

[1] *Abbreviations used in this paper:* ACAT, acyl CoA:cholesterol acyl transferase; ADRP, adipocyte differentiation related protein; BFA, brefeldin A; CE, cholesteryl ester; DTAF, dichlorotriazinylaminofluorescein; FRT, Fischer rat thyroid; IF, immunofluorescence; LPDS, lipoprotein-depleted serum; TG, triacylglyceride.
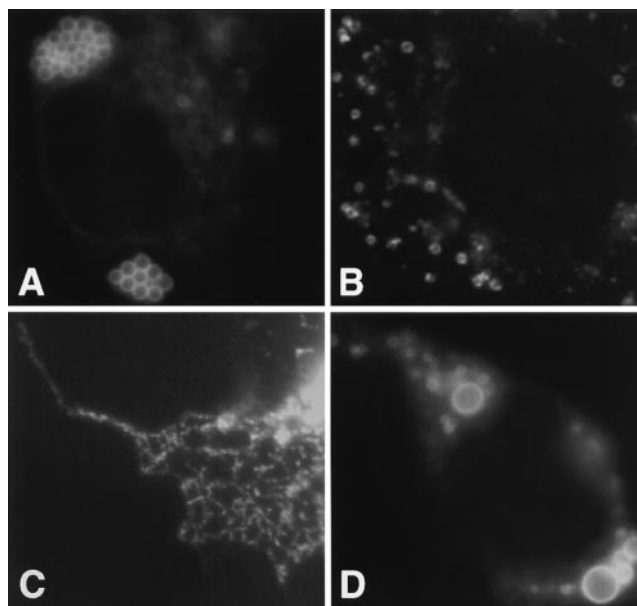
Figure 1. Localization of Cav–KKSL. Cav–KKSL in transiently transfected FRT (A and B) or COS (C and D) cells was visualized by IF.

Reduction of Cholesteryl Ester (CE) Levels

Day 0, FRT cells were transferred to Coon's F12 media containing 10% lipoprotein-depleted serum (LPDS; Goldstein et al., 1983) or cells were left in control media. Day 5, cells were transfected with Cav–KKSL. The ACAT inhibitor CP 113,818 (2 μg/ml) was added to the dish containing LPDS 24–36 h before harvest. Cells were fixed for detection of Cav–KKSL by IF or were subjected to lipid extraction to quantitate CE.

Quantitation of CE and Triacylglyceride (TG)

In Fig. 6 A, lipids in confluent cell monolayers in 35-mm dishes were extracted as reported previously (Brown and Rose, 1992). In Fig. 7 A, cells were seeded in parallel 60-mm dishes (for lipid extraction) and 35-mm dishes with coverslips (for IF, staining for Cav–KKSL and counterstaining with DAPI to determine the percent of cells that were transfected). For transient transfections, the same transfection mixture was used for both dishes. Nonpolar lipids from cells in confluent 60-mm dishes were extracted with hexane/isopropyl alcohol 3:2 (Underwood et al., 1998). In Figs. 6 A and 7 A, extracted lipids (100% of the FRT and HEK 293 extracts or 10% of the COS extracts) were separated by high-performance thin-layer chromatography (HP-TLC) using hexane/isopropyl ether/acetic acid 65:35:2, and visualized by charring and quantitated by densitometric scanning and comparison to standards on the same plate as described (Brown and Rose, 1992). Cholesterol, not expected to accumulate in lipid droplets, was also scanned as an internal control.

Results

Cav–KKSL Exhibits a Novel Localization

Cav–KKSL was expressed transiently in FRT cells, which lack endogenous caveolin-1 and caveolae (Lipardi et al., 1998), or in COS cells, which express caveolin-1 endogenously (Fig. 1). Cav–KKSL was not detected in the plasma membrane, suggesting that direct transport from the ER to the plasma membrane (Uittenbogaard et al., 1998) is at most a minor pathway. In some cells, Cav–KKSL was detectable in the ER (Fig. 1 C). In most cells, however, the protein accumulated predominantly on the surface of spherical structures that varied in size and were often, but
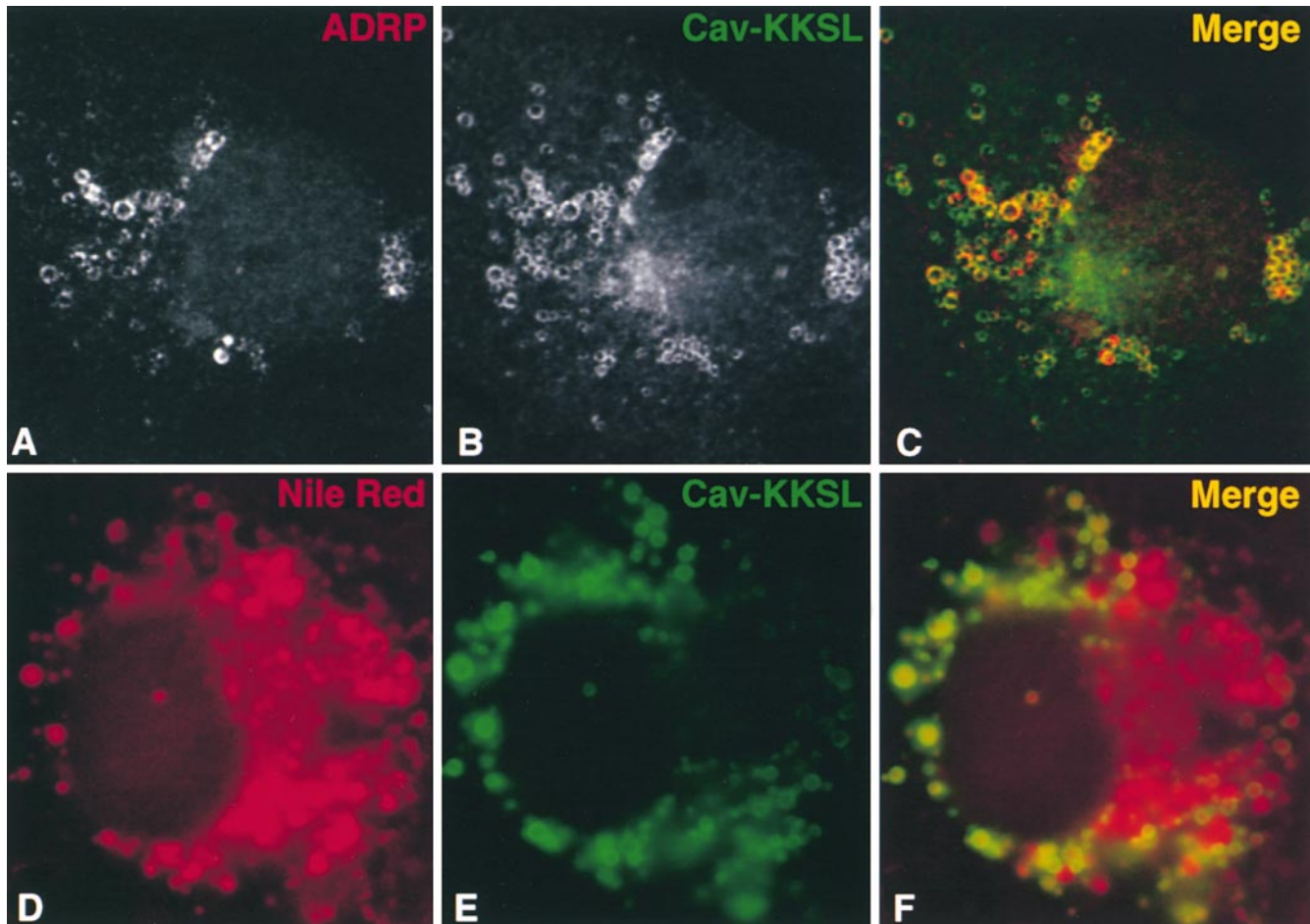
Figure 2. Colocalization of Cav–KKSL, ADRP, and Nile red staining. Endogenous ADRP (A) and transiently expressed Cav–KKSL (B) in a COS cell were visualized by IF. C, Merged image of A and B. Nile red stain (D) and IF visualization of Cav–KKSL (E) in a transiently transfected FRT cell. F, Merged image of D and E.

not always, clustered together. Cav–KKSL was also seen in these structures when expressed in HEK-293 and CHO cells, although ER staining was more prominent than in the other two lines (not shown).

Cav–KKSL-positive Structures Are Lipid Storage Droplets

To determine whether the Cav–KKSL-positive structures were lipid storage droplets, Cav–KKSL-expressing FRT cells were double-labeled with antibodies to Cav–KKSL and with either Nile red or with antibodies to ADRP. Nile red stained the lipid droplet cores, whereas both Cav–KKSL and ADRP were localized to the surface of the droplets (Fig. 2). In some transfected cells, almost all Nile-red positive droplets were also positive for Cav–KKSL. In others (Fig. 2 F), some droplets stained only for Nile red.

An Internal Deletion Mutant of Caveolin-1 Accumulates in Lipid Droplets

We also examined the localization of Cav–ΔN2, a mutant made for unrelated studies, that lacks residues 46–95 of caveolin-1, including almost the entire downstream half of the NH$_2$-terminal hydrophilic domain. In some cells, Cav–ΔN2 was present in the Golgi apparatus (identified as a

perinuclear structure labeled with FITC-lens lectin, not shown). However, in most cells the protein was present in lipid droplets, identified by their characteristic morphology. Both patterns are evident in the cell shown in Fig. 3 A. The presence of Cav–ΔN2 in lipid droplets showed that the KKSL tag is not required for the accumulation of Cav–KKSL in the droplets. We also conclude that residues 46–95, which include most of the caveolin scaffolding domain previously reported to mediate binding of caveolin-1 to other proteins (Smart et al., 1999), are not required for lipid droplet targeting.

Accumulation of Caveolin-1 in the ER with Brefeldin A Targets the Protein to Lipid Droplets

What might Cav–KKSL and Cav–ΔN2 have in common that is not shared by caveolin-1, that could explain the accumulation of both proteins in lipid droplets? One possibility is accumulation to unusually high levels in the ER. Retrieval of Cav–KKSL to the ER should increase its concentration there. Cav–ΔN2 might fold slowly, or might lack a domain required for interaction with a cargo receptor and efficient packaging into transport vesicles. Either effect would retard transport of the protein from the ER. In contrast, caveolin-1 is probably normally
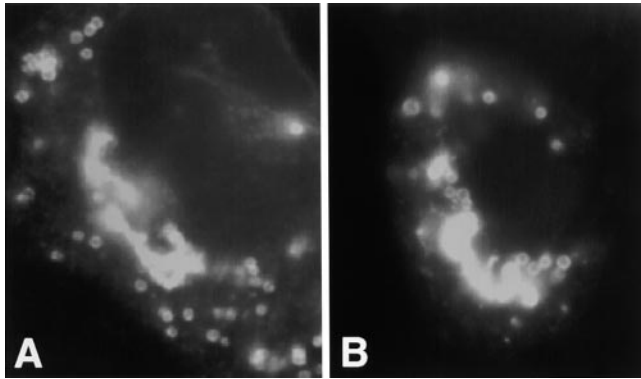
Figure 3. Localization of Cav–ΔN2 and caveolin-2. IF localization of Cav–ΔN2 (A) and caveolin-2 (B) in transiently transfected FRT cells. The Golgi apparatus was overexposed to show the droplets.

transported efficiently from the ER, never reaching a high concentration there.

To determine whether ER accumulation is sufficient to target caveolin-1 to lipid droplets, we incubated FRT cells transiently transfected with caveolin-1 for 5 h in BFA to collapse the Golgi apparatus into the ER (Lippincott-Schwartz et al., 1989). Both Golgi apparatus-localized and newly synthesized caveolin-1 should accumulate in the ER during BFA treatment. IF localization of caveolin-1 in control, untreated cells showed the expected punctate plasma membrane staining and Golgi apparatus staining (Fig. 4 A). (Golgi apparatus staining of caveolin-1 in transfected FRT cells was often more pronounced than in cells that express caveolin-1 endogenously.) The Golgi apparatus, detected with lens lectin, had the expected morphology in control cells (Fig. 4 D). As expected, lens lectin staining assumed a diffuse ER-like pattern after BFA treat-

ment (Fig. 4 E). Caveolin-1 was detectable in lipid droplets in about half of the transfected cells after BFA treatment (Fig. 4 B), and showed a punctate or reticular pattern in the other cells (not shown). BFA also induced accumulation of GFP-tagged caveolin-1 in lipid droplets in living CHO cells (not shown).

What is the fate of caveolin-1 in lipid droplets? One possibility is that caveolin-1 normally passes through lipid droplets while cycling through the cell. Alternatively, caveolin-1 may not normally enter the droplets. If endogenous caveolin-1 normally travels through the droplets, it must exit from them rapidly, as the protein is not detected there at steady-state. To determine how rapidly caveolin-1 moves out of the droplets, we took advantage of the fact that the known effects of BFA are readily reversible upon drug washout. We incubated FRT cells for 5 h with BFA, washed out the drug, and incubated for 3 h before fixing and staining for caveolin-1. The Golgi apparatus reassumed its normal morphology in this time (Fig. 4 F). However, caveolin-1 was still observed in lipid droplets in about half the transfected cells (Fig. 4 C). Thus, transport of caveolin-1 out of lipid droplets after BFA washout was slow or did not occur, suggesting that the droplets are not on the normal transport pathway.

Overexpressed Caveolin-2 Accumulates in Lipid Droplets and in the Golgi Apparatus

Endogenous or stably overexpressed caveolin-2 accumulates in the Golgi apparatus in FRT cells (Mora et al., 1999). We found that HA-tagged caveolin-2 also accumulated in the Golgi apparatus in transiently transfected FRT cells (Fig. 3 B). Surprisingly, caveolin-2 was also detected in lipid droplets in 30–50% of the transiently transfected cells (Fig. 3 B). GFP-tagged caveolin-2 was also seen in lipid droplets in living CHO cells (not shown). By contrast, GFP–caveolin-1 was not seen in lipid droplets in CHO
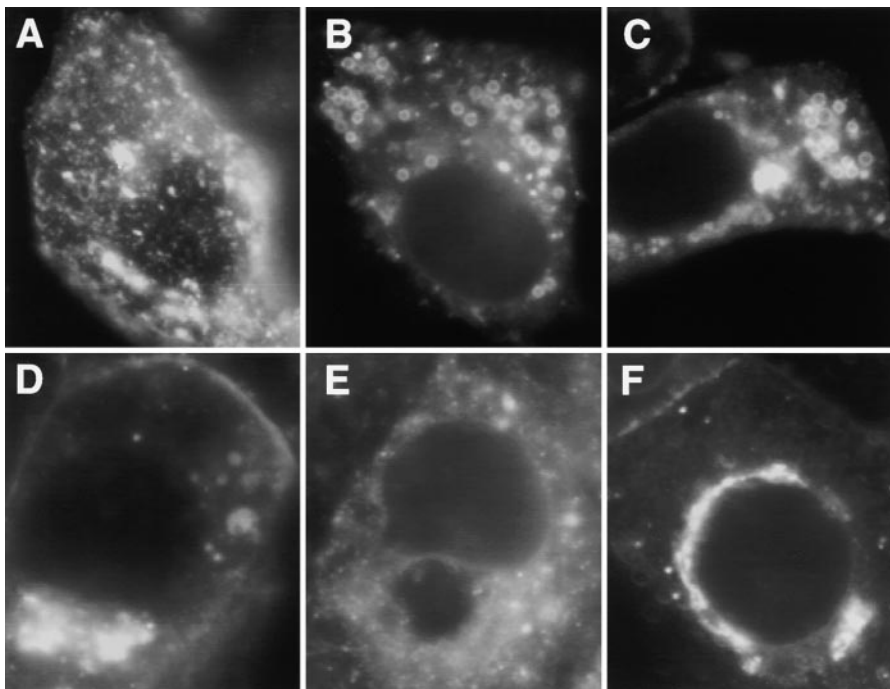

Figure 4. Effect of BFA on caveolin-1 localization. FRT cells were transiently transfected with HA/myc-tagged caveolin-1. Cells were either left untreated (A and D) or BFA-treated for 5 h (B, C, E, and F). BFA-treated cells were either fixed immediately (B and E) or were incubated at 37°C for 3 h in normal growth media after washing out BFA before fixation (C and F). Caveolin-1 was visualized by IF (A–C). Golgi apparatus morphology in cells on separate coverslips was monitored using FITC-lens lectin (D–F). Experiments in which caveolin-1 and lens lectin staining were visualized in the same cells gave similar results (not shown).
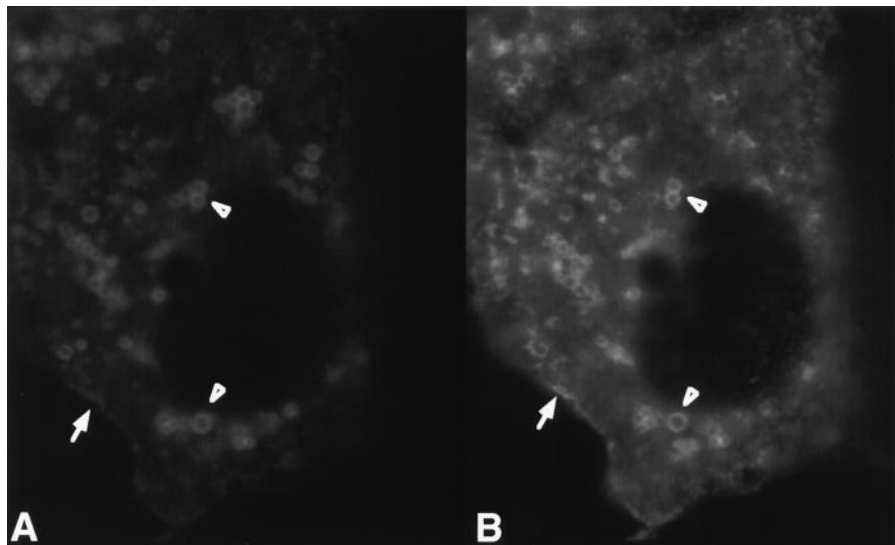
Figure 5. Partial recruitment of caveolin-1 to lipid droplets by Cav–KKSL. FRT cells were transiently cotransfected with Cav–KKSL and HA/Myc-tagged caveolin-1 and double-labeled with anti-caveolin-1 antibodies and Texas-red secondary antibodies (A; to detect both proteins) and anti-HA antibodies and DTAF secondary antibodies (B; to detect the wild-type protein specifically). Arrow, plasma membrane staining; arrowheads, lipid droplets.

cells, and overexpressed caveolin-1 was only very occasionally (<0.1% of transfected cells) seen in lipid droplets in FRT cells without BFA treatment (not shown). We conclude that caveolin-2, as well as caveolin-1, can enter the droplets. Caveolin-2, unlike caveolin-1, can readily be targeted to the droplets by overexpression. Inefficient transport of caveolin-2 through the secretory pathway (Mora et al., 1999) may cause this targeting. The similar localization of overexpressed Cav–ΔN2 and caveolin-2 (Fig. 3, A and B) suggests that folding or transport rates of the two proteins may be similarly slow.

Caveolin-1 Accumulates in Lipid Droplets When Coexpressed with Cav–KKSL

If the presence of high levels of caveolin in the ER is sufficient to cause lipid droplet targeting, then coexpression with Cav–KKSL, which accumulates in the ER, should divert some caveolin-1 to the droplets. To test this idea, myc-tagged Cav–KKSL and HA/myc-tagged caveolin-1 were transiently coexpressed in FRT cells. As expected, anticaveolin antibodies, which recognized both proteins, stained both lipid droplets and the plasma membrane (Fig. 5 A). Anti-HA antibodies, which recognized only caveolin-1, gave a similar staining pattern (Fig. 5 B). Thus, coexpression with Cav–KKSL redirected some caveolin-1 to lipid droplets. This targeting might result from accumulation of caveolin in the ER, as we have suggested. Alternatively, it might result from heterooligomerization of caveolin-1 and Cav–KKSL.

Cholesterol Ester Depletion Does Not Affect the Localization of Cav–KKSL

ACAT, which converts free cholesterol to CE that accumulates along with TG in lipid storage droplets, is localized in the ER. As caveolin-1 binds cholesterol and can associate with cholesterol-rich lipid microdomains (Smart et al., 1999), we wondered whether CE were required for targeting of Cav–KKSL to lipid droplets, possibly through tight binding of Cav–KKSL to CE. To test this model, we determined whether inhibiting ACAT affected Cav–KKSL localization. Cellular CE levels were reduced by 70–80% by growth in LPDS and CP 113,818 treatment
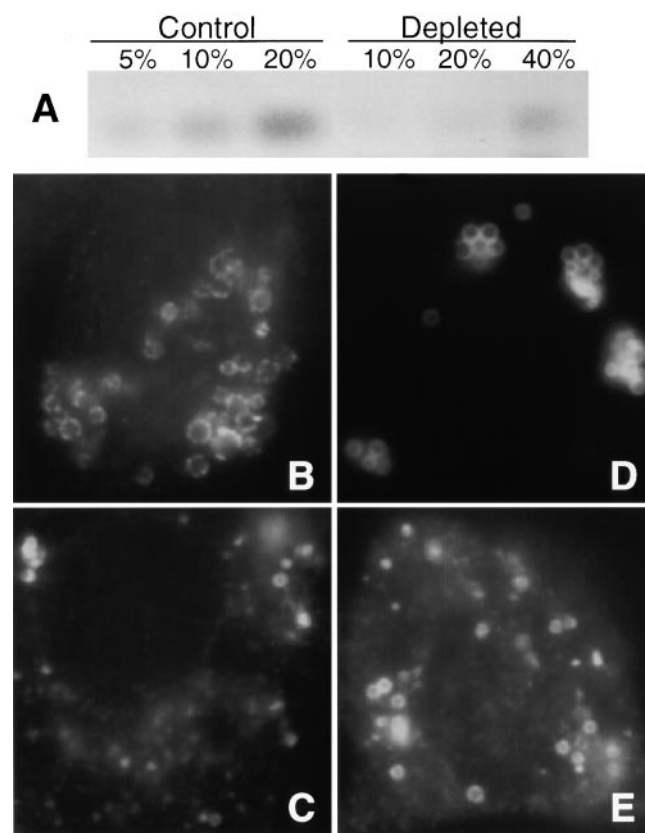

Figure 6. CE depletion does not affect Cav–KKSL localization. A, FRT cells in 100-mm dishes were grown as usual (Control) or depleted of CE as described in Materials and Methods (Depleted). The indicated fraction of the total lipids isolated from each plate was then analyzed by HP-TLC as in Materials and Methods. The charred CE bands are shown. The levels of other lipids were not affected (not shown). B–E, Cav–KKSL in CE-depleted FRT cells transiently expressing Cav–KKSL was visualized by IF. The range of staining patterns was identical to that in control cells processed in parallel (not shown).
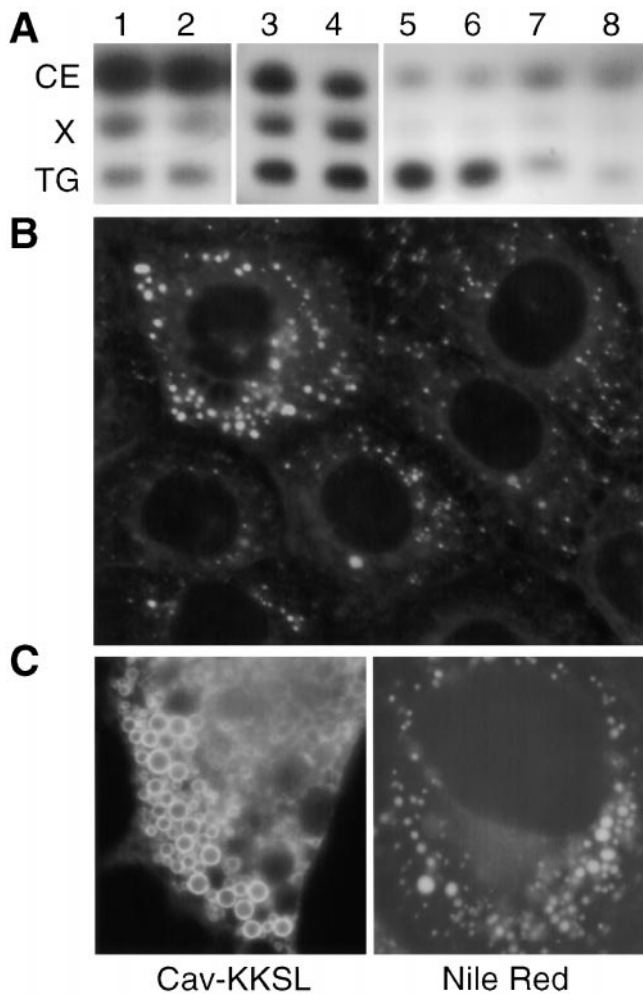
Figure 7. Effect of Cav–KKSL on lipid droplets. A, Lipids from various cell types were separated by HP-TLC and visualized by charring. Lanes 1 and 2 are from a separate plate. Positions of CE, TG, and unidentified lipid X are indicated. Cells used and (percent of cells expressing Cav–KKSL); 1, G418-resistant FRT cells; 2, FRT clone B4 stably expressing Cav–KKSL (19%); 3, transient FRT/vector; 4, transient FRT/Cav–KKSL (32%); 5, COS/vector; 6, COS/Cav–KKSL (36%); 7, HEK 293/vector; 8, HEK 293/Cav–KKSL (53%). Only 10% of the COS cell extracts (lanes 5 and 6) were loaded on the plate. B, Untransfected FRT cells were stained with Nile red. C, COS cells were transiently transfected with Cav–KKSL, detecting the protein by IF (left), or were stained with Nile red (right; a cell with large droplets).

(Fig. 6 A). Cells were then transfected with Cav–KKSL and examined by IF (Fig. 6, B–E). Cav–KKSL localization appeared unaffected by CE reduction. We conclude that high levels of newly synthesized CE are not required for targeting of Cav–KKSL to lipid droplets.

Effect of Cav–KKSL Expression on Lipid Droplets

We first determined whether Cav–KKSL affected cellular levels of TG and CE, the major storage lipids in mammalian cells. The behavior of perilipins, proteins that coat lipid droplets in adipocytes, provides a precedent for this idea. Overexpression of perilipins inhibits TG hydrolysis, causing TG to accumulate (Brasaemle et al., 2000).

To this end, we first selected stable Cav–KKSL transfectants from FRT cells. Generating these lines was difficult, and only two were obtained. Furthermore, Cav–KKSL was detectable by IF in only 10–20% of the cells in each line, although caveolin-1 was detectable in essentially all cells in a stably transfected FRT cell line (Lipardi et al., 1998) (not shown). These results raised the possibility that Cav–KKSL was harmful to cells, and that the two stable transfectants were abnormal. For this reason, we also examined the effect of transient Cav–KKSL expression on TG and CE levels in FRT, COS, and HEK 293 cells. Cav–KKSL expression had no significant effect on TG or CE levels in any of these cells (Fig. 7 A). As the transient transfection efficiency was ∼30–50% (see legend to Fig. 7 A), a large effect should have been detectable.

To determine whether Cav–KKSL affected lipid droplet morphology, we compared Cav–KKSL-positive droplets in transiently transfected COS and FRT cells with Nile red-positive droplets in untransfected cells. Lipid droplets were present in untransfected cells (Fig. 7, B and C). Droplet size and number varied widely among cells, especially in FRT cells (Fig. 7 B). However, in these cells the range appeared similar to that in Cav–KKSL-positive cells after transient transfection (Figs. 1, 2, and 6). Although this suggested that Cav–KKSL did not affect lipid droplet structure, the heterogeneity made this difficult to determine precisely. However, lipid droplets were clustered in many (but not all) Cav–KKSL-positive cells (Figs. 1 and 6), but not in untransfected cells (Fig. 7). Interaction between Cav–KKSL molecules on adjacent droplets may cause them to cluster.

In COS cells, Cav–KKSL-positive lipid droplets looked similar to Nile red positive droplets in many cells. However, the largest droplets appeared larger than the largest droplets seen in control cells (Fig. 7 C; also see Fig. 1 D), suggesting that Cav–KKSL can increase lipid droplet size.

Discussion

How Caveolins Might Access Lipid Droplets

Lipid droplet biogenesis is not well understood (Londos et al., 1999; Murphy and Vance, 1999). However, the prevailing model rationalizes how caveolins (but not most other membrane proteins) might be able to enter the droplets (Fig. 8). Lipid droplets are derived from the ER, where TG and CE are synthesized, and are thought to be surrounded by a phospholipid monolayer (Londos et al., 1999; Murphy and Vance, 1999). These observations suggest that neutral lipids accumulate in the hydrophobic core of the bilayer, forming a bulge that eventually buds from the ER membrane to form a free droplet. Accumulation of neutral lipids in the bilayer core would initially force opposite leaflets of the bilayer apart, increasing bilayer thickness. Such a thickened bilayer would not be able to accommodate transmembrane proteins that have hydrophilic domains on both sides of the membrane, and these proteins would be excluded from the forming droplets. Caveolins, by contrast, lack luminal hydrophilic domains, and could diffuse freely between the ER membrane and the monolayer surrounding the nascent droplet. Thus, caveolins would not need to dissociate from the ER membrane
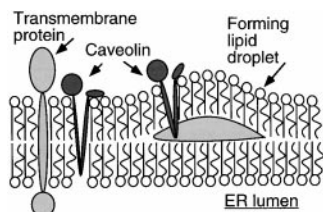
Figure 8. How caveolin-1 might enter lipid droplets. Neutral lipids may accumulate in the interior of the ER bilayer, making a bulge that eventually buds into the cytoplasm to form a droplet surrounded by an ER-derived phospholipid monolayer. This process would drive opposite ER membrane monolayers apart, effectively thickening the hydrophobic portion of the membrane. Most membrane proteins, which contain hydrophilic domains on both sides of the bilayer, could not be accommodated in this environment and would be excluded from the forming droplets. By contrast, caveolin-1 has no luminal hydrophilic domain and could easily diffuse laterally between the ER membrane proper and the monolayer surrounding the nascent droplets.

and expose their hydrophobic domains to the cytosol to enter the droplets. This model suggests that caveolins can enter lipid droplets only while they are forming, and are still in contact with the ER. Consistent with this idea, we noticed that in some transfected cells, only some of the Nile red positive droplets contained Cav–KKSL (Fig. 2). We speculate that the Cav–KKSL-negative droplets budded from the ER before expression of Cav–KKSL started.

Why Might Caveolins Sometimes Accumulate in Lipid Droplets?

Our results suggest that accumulation of caveolins in the ER leads to lipid droplet targeting, and we favor this model. However, an alternate possibility is that transport of caveolins to the ER via a retrograde pathway somehow leads to lipid droplet targeting. Retrograde transport is expected for Cav–KKSL, as KKXX-tagged proteins are known to follow this route (Letourneur et al., 1994). Caveolins in BFA-treated cells may also undergo retrograde transport. Because BFA does not inhibit COPII-coated vesicle formation (Bednarek et al., 1995), COPII-coated vesicles may continue to bud from the ER and possibly even reach the ER to Golgi intermediate complex (ERGIC; which does not collapse into the ER; Schweizer et al., 1993) during BFA treatment. If so, the cargo proteins must be rapidly recycled to the ER. Finally, misfolded proteins bound to chaperones can also be retrieved from the ERGIC and Golgi apparatus to the ER (Hammond and Helenius, 1994). Inefficient transport of caveolin-2 in the absence of caveolin-1 and of Cav–ΔN2 suggests that these proteins may not fold properly.

Although we do not know how ER accumulation of caveolins might lead to an apparent concentration of the proteins in lipid droplets, several possible explanations can be imagined. First, caveolins might have a high affinity for lipid droplets, either through binding to a protein or lipid in the droplets, or through preference for the physical state of the droplet phospholipid monolayer or neutral lipid core. Efficient packaging of caveolins into transport vesicles might normally prevent entry into the droplets. Accumulation in the ER might saturate some component of the transport machinery, possibly a specific cargo receptor, giving the protein time to access the droplets. Alternatively, accumulation of caveolins in the ER might change the

properties of the ER membrane. As caveolin-1 binds cholesterol (Smart et al., 1999), this might occur through accumulation of cholesterol in the ER. The altered properties might increase the affinity of caveolins for lipid droplets, either by changing the physical properties of the membrane, or by inducing a conformational change in caveolins.

Intriguingly, oleosins, a family of plant lipid-droplet proteins (Murphy and Vance, 1999), have a similar topology to caveolins, with a central hydrophobic domain flanked by two cytoplasmic domains. Lipid droplet targeting signals are contained in the hydrophobic domain (Abell et al., 1997). Further work will show whether the unusual topology, the hydrophobic domain, or any specific sequences are required for lipid droplet targeting and/or accumulation of caveolins.

Physiological Relevance of Lipid Droplet Targeting of Caveolins

We do not know whether caveolins normally pass through lipid droplets during biosynthetic transport or intracellular cycling. If they do, they must exit the droplets rapidly, as they are not normally detected there. Thus, our finding that caveolin-1 remained in lipid droplets long after BFA washout, suggesting that transport of caveolins from the droplets is slow, implies that caveolins do not normally pass through the droplets. However, it remains possible that caveolins may be transported to the droplets under as-yet-unidentified conditions.

We do not know how (or whether) caveolins function in the droplets. Cav–KKSL appeared to increase the size and possibly the abundance of lipid droplets in some COS cells, which contain much more TG than the other cells we examined. We did not detect an effect of Cav–KKSL on CE or TG levels in a population of transiently transfected cells. However, our assay might not have detected an increase if Cav–KKSL induced lipid accumulation in a subset of transfected cells. Such an effect could occur if Cav–KKSL sterically blocked access of lipases to the droplets, as is thought to occur in cells overexpressing perilipins (Brasaemle et al., 2000). Accumulation of caveolins in lipid droplets might also affect cholesterol trafficking, as shown for a dominant-negative caveolin mutant in the accompanying paper (Pol et al., 2001, this issue).

In any case, the unusual targeting we have identified here may provide clues to the puzzle of how caveolins normally interact with lipids in caveolae and other membranes.

References

Abell, B.M., I.A. Holbrook, M. Abenes, D.J. Murphy, M.J. Hills, and M.M. Moloney. 1997. Role of the proline knot motif in oleosin endoplasmic reticulum topology and oil body targeting. *Plant Cell*. 9:1481–1493.

Arni, S., S.A. Keitbaugh, A.G. Ostermeyer, and D.A. Brown. 1998. Association

of GAP-43 with detergent-resistant membranes requires two palmitoylated cysteine residues. *J. Biol. Chem.* 273:28478–28485.

Bednarek, S.Y., M. Ravazzola, M. Hosobuchi, M. Amherdt, A. Perrelet, R. Schekman, and L. Orci. 1995. COPI- and COPII-coated vesicles bud directly from the endoplasmic reticulum in yeast. *Cell.* 83:1183–1196.

Brasaemle, D.L., B. Rubin, I.A. Harten, J. Gruia-Gray, A.R. Kimmel, and C. Londos. 2000. Perilipin A increases triacylglycerol storage by decreasing the rate of triacylglycerol hydrolysis. *J. Biol. Chem.* 275:38486–38493.

Brown, D.A., and J.K. Rose. 1992. Sorting of GPI-anchored proteins to glycolipid-enriched membrane subdomains during transport to the apical cell surface. *Cell.* 68:533–544.

Dietzen, D.J., W.R. Hastings, and D.M. Lublin. 1995. Caveolin is palmitoylated on multiple cysteine residues: palmitoylation is not necessary for localization of caveolin to caveolae. *J. Biol. Chem.* 270:6838–6842.

Fra, A.M., E. Williamson, K. Simons, and R.G. Parton. 1995. De novo formation of caveolae in lymphocytes by expression of VIP21-caveolin. *Proc. Natl. Acad. Sci. USA.* 92:8655–8659.

Goldstein, J.L., S.K. Basu, and M.S. Brown. 1983. Receptor-mediated endocytosis of low-density lipoprotein in cultured cells. *Methods Enzymol.* 98:241–260.

Hammond, C., and A. Helenius. 1994. Quality control in the secretory pathway: retention of a misfolded viral membrane glycoprotein involves cycling between the ER, intermediate compartment, and Golgi apparatus. *J. Cell Biol.* 126:41–52.

Kurzchalia, T.V., and R.G. Parton. 1999. Membrane microdomains and caveolae. *Curr. Opin. Cell Biol.* 11:424–431.

Kurzchalia, T.V., P. Dupree, R.G. Parton, R. Kellner, H. Virta, M. Lehnert, and K. Simons. 1992. VIP21, a 21-kD membrane protein, is an integral component of trans-Golgi-network–derived transport vesicles. *J. Cell Biol.* 118:1003–1014.

Letourneur, F., E.C. Gaynor, S. Hennecke, C. Démollière, R. Duden, S.D. Emr, H. Riezman, and P. Cosson. 1994. Coatomer is essential for retrieval of dilysine-tagged proteins to the endoplasmic reticulum. *Cell.* 79:1199–1207.

Lipardi, C., R. Mora, V. Colomer, S. Paladino, L. Nitsch, E. Rodriguez-Boulan, and C. Zurzolo. 1998. Caveolin transfection results in caveolae formation but not apical sorting of glycosylphosphatidylinositol (GPI)-anchored pro-teins in epithelial cells. *J. Cell Biol.* 140:617–626.

Lippincott-Schwartz, J., L.C. Yuan, J.S. Bonifacino, and R.D. Klausner. 1989. Rapid redistribution of Golgi proteins into the ER in cells treated with brefeldin A: evidence for membrane cycling from Golgi to ER. *Cell.* 56:801–813.

Londos, C., D.L. Brasaemle, C.J. Schultz, J.P. Segrest, and A.R. Kimmel. 1999. Perilipins, ADRP, and other proteins that associate with intracellular neutral lipid droplets in animal cells. *Semin. Cell Dev. Biol.* 10:51–58.

Mora, R., V.L. Bonilha, A. Marmorstein, P.E. Scherer, D. Brown, M.P. Lisanti, and E. Rodriguez-Boulan. 1999. Caveolin-2 localizes to the Golgi complex but redistributes to plasma membrane, caveolae, and rafts when co-expressed with caveolin-1. *J. Biol. Chem.* 274:25708–25717.

Murphy, D.J., and J. Vance. 1999. Mechanisms of lipid-body formation. *Trends Biochem. Sci.* 24:109–115.

Pol, A., R. Luetterforst, M. Lindsay, S. Heino, E. Ikonen, and R.G. Parton. 2001. A caveolin dominant negative mutant associates with lipid bodies and induces intracellular cholesterol imbalance. *J. Cell Biol.* 152:1057–1070.

Schweizer, A., M. Ericsson, T. Bächi, G. Griffiths, and H.-P. Hauri. 1993. Characterization of a novel 63 kDa membrane protein: implications for the organization of the ER-to-Golgi pathway. *J. Cell Sci.* 104:671–683.

Smart, E.J., G.A. Graf, M.A. McNiven, W.C. Sessa, J.A. Engelman, P.E. Scherer, T. Okamoto, and M.P. Lisanti. 1999. Caveolins, liquid-ordered domains, and signal transduction. *Mol. Cell. Biol.* 19:7289–7304.

Tanaka, M., and W. Herr. 1990. Differential transcriptional activation by Oct-1 and Oct-2: interdependent activation domains induce Oct-2 phosphorylation. *Cell.* 60:375–386.

Uittenbogaard, A., Y.-s. Ying, and E.J. Smart. 1998. Characterization of a cytosolic heat-shock protein–caveolin chaperone complex. Involvement in cholesterol trafficking. *J. Biol. Chem.* 273:6525–6532.

Underwood, K.W., N.L. Jacobs, A. Howley, and L. Liscum. 1998. Evidence for a cholesterol transport pathway from lysosomes to endoplasmic reticulum that is independent of the plasma membrane. *J. Biol. Chem.* 273:4266–4274.

Warner, G.J., G. Stoudt, M. Bamberger, W.J. Johnson, and G.H. Rothblat. 1995. Cell toxicity induced by inhibition of acyl coenzyme A:cholesterol acyltransferase and accumulation of unesterified cholesterol. *J. Biol. Chem.* 270:5772–5778.